Large and continuous tuning of the work function of indium tin oxide using simple mixing of self-assembled monolayers

Giovanni Ligorio,[a,1] Nicolas Zorn Morales[a] and Emil J. W. List-Kratochvil [a,b]

a) *Humboldt-Universität zu Berlin, Institut für Physik, Institut für Chemie & IRIS Adlershof Brook-Taylor-Straße 6, 12489 Berlin, Germany.*
b) Helmholtz-Zentrum Berlin für Materialien und Energie GmbH, Brook-Taylor-Straße 6, 12489 Berlin, Germany.

Self-assembled monolayers (SAMs) have been extensively investigated in opto-electronic applications, such as organic light emitting diodes (OLEDs). The SAM is used to tune the energy level alignment by allowing ohmic contact at the interface between electrodes and organic semiconductors. To achieve the required energy level alignment and modify the electrode work function, molecules carrying a permanent dipole are chemically grafted at the electrode surface. Typically, the electrodes are modified by choosing one specific molecule carrying the appropriate dipole to achieve the desired (discrete) work function value. In this contribution, we propose a simple way to continuously tune the work function over almost 1 eV and demonstrate this on the most commonly used transparent electrode, namely indium tin oxide (ITO). The continuous tuning is achieved by selecting two molecules able to form SAMs, each carrying a different permanent dipole. Solutions comprising the molecules are mixed at different relative concentrations and deposited on the ITO surface. The composition of the resulting densely packed mixed SAM is directly related to the composition of the initial mixing in solution. The effect of the SAM on the ITO electronic landscape was analysed by various surface sensitive measurements. Furthermore, the differently functionalized transparent electrodes have been integrated in prototypical OLEDs. Through electrical characterization we confirm the ability to continuously tune the carrier injection and thereby improve the luminescence.

Transparent electrodes play a fundamental role as electrode materials in opto-electronic device applications such as organic light-emitting diodes (OLEDs) or organic photovoltaic devices. Among the metal oxides commonly employed, indium tin oxide (ITO) is the most widely used transparent anode electrode. However, its work function (WF) is commonly found to be in the range of 4.5 eV - 4.8 eV [1–4] and thus does not allow for efficient hole injection into the highest occupied molecular orbital (HOMO) of most of the materials used as hole transport materials.[3,4]

Several physical/chemical treatments have been developed to modify the interface with the goal of improving the hole injection. These processes aim to reduce the energy barrier at the interface by adjusting the energy levels of the electrode to match the transport energy levels of the organic semiconductor. In addition to surface modification by means of oxygen plasma or UV-ozone treatment, several organic and inorganic interlayers (e.g. polyethylenimine, lithium fluoride, chlorine) have been employed at the interface.[3,5–9]

Alternatively, covalently bound self-assembled monolayers (SAMs) carrying a permanent dipole group have also become a common tool to tune the energy level.[10–13] Several comprehensive works demonstrate that

---

[1] *giovanni.ligorio@hu-berlin.de*

it is possible to fine tune the energy level over a large energy window (1 eV) and improve drastically the carrier injection. In all these contributions, the WF of the electrode is modified by choosing one specific molecule carrying the appropriate dipole to achieve the desired WF.

When this approached is employed, the electrode surface is fully saturated with the SAM interlayer. A partial coverage would allow for a continuous tuning between the intrinsic WF value of the electrode and the value determined upon SAM functionalization. Conceptually, the concentration of the SAM molecules at the interface could be controlled by varying the exposure time to the employed molecule. However, given the dynamic nature of the SAM formation process, the immersion time cannot be used as a reliable parameter for controlling the density of molecules at the interface. Too many parameters influence the chemisorption dynamics, such as temperature, polarity of solvent, and substrate preparation and pretreatment, which, in case of metal oxide and phosphonic acid, ultimately influences the density of -OH groups at the interface onto which PAs bind. Furthermore, at low coverage the SAM molecules are not randomly dispersed at the electrode interface but rather form islands that leave some parts of the electrode uncovered and other parts covered.[14] To avoid this lack in control, a possible solution is to ensure saturated molecular coverage at the interface via mixing two molecules carrying different dipoles By varying the concentration ratio of two molecules in the SAM, it has been shown that it is possible to fine tune the final WF. This has been shown on metals as Au and Ag.[15,16]

In this contribution, we adopt this approach on the more relevant electrode for opto-electronic applications mentioned above, ITO. The formation of a homogenous and dense SAM is achieved by soaking ITO in SAM solutions comprising different concentration ratios of two molecules. A crucial aspect in this study is the evaluation of the effective mixture of molecules on the substrate with respect to the nominal mixture of molecules in the SAM solution.

For the SAM, we employed octylphosphonic acid (OPA) and 1H,1H,2H,2H-perfluorooctanephosphonic acid (FOPA). Both molecules carry a phosphonic acid (PA) group which serves as ideal anchoring group for metal oxides. Additionally, the chemical backbone structure of both molecules is equally linear, providing the possibility of enhanced molecule-molecule interaction and reducing steric hindrance during the formation of densely packed SAM. By combining an extensive examination of the functionalized ITO interface properties and fabrication of OLEDs comprising the mixed SAMs, we find that the WF of ITO can be continuously tuned by simply varying the ratio between OPA and FOPA.

For the fabrication of the SAM-functionalized electrodes, ITO-coated glass substrates (sheet resistance = 20 Ω/□; *Psiotec*) were cleaned by sequential sonication in acetone and isopropyl alcohol, followed by 5 minutes in oxygen plasma. For the deposition of SAM on the substrates, two stock solutions were prepared: both OPA and FOPA molecules (*Sigma Aldrich*) were dissolved in anhydrous tetrahydrofuran (THF) with a concentration of 1 mM. The two solutions were mixed by volume in order to generate 5 mixed solutions with different OPA:FOPA percentage ratio, namely 100:0, 75:25, 50:50, 25:75 and 0:100. SAM formation on the ITO is based on a procedure that has been optimized for phosphonic acids on metal oxides and extensively reported previously.[17–20] The procedure follows 3 steps: (*i*) soaking of the substrate in SAM solution for 1 hour; (*ii*) annealing in air for 10 minutes on a hot plate at 80°C to promote chemisorption; (*iii*) 5 minutes sonication in THF to dissolve the molecules not chemically bound.

The formation of the SAMs was initially assessed via the change of the sample's surface energy evaluated by the contact angle of a probe liquid. Static contact angle (CA) measurements were carried out (DSA100E from *Krüss*) using the sessile drop method with de-ionised water. Figure 1-a displays the pictures of the water drop on the substrates. The CA value reported above the images is calculated as average between six drops on each sample.
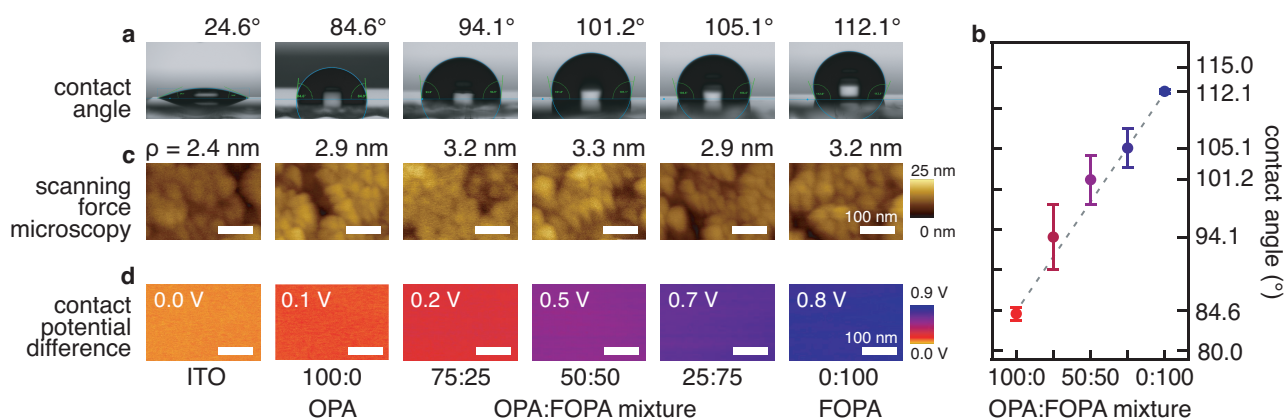
Figure 1. The water contact angle (a) increases as a function of the amount of FOPA in the SAM. The measured angles correlate with the nominal amount of FOPA (b). No morphological changes are observed in the SFM images (c) beside a slight increase of surface roughness ρ. The contact potential difference (d) indicates an increase of the WF as the nominal FOPA amount increases.

As expected, the bare ITO displays the lowest value, 24.6° ± 1.0. Upon functionalization with pure OPA (100:0), the CA abruptly increases to 84.6 ± 0.8°. This clearly indicates that the substrate was modified. The measured CA on the ITO functionalized with the mixed OPA:FOPA ratio (75:25, 50:50 and 25:75) reveal a steady increase as a function of the higher nominal amount of FOPA. The highest CA value (112.1° ± 0.4°) is measured with pure FOPA (0:100). This monotonic increase of the CA is expected considering the higher hydrophobicity induced by the fluorination of the alkane chain in FOPA. The correlation between CA and nominal ratio is graphically depicted in Figure 1-b and is confirmed by the good agreement between the experimental data and line which serves as guide for the eye. The CA measurements give a first indication that the composition of the SAM on the ITO surface is related to the OPA:FOPA ratio.

To inspect possible morphological changes induced by the phosphonic anchoring group at the surface of ITO, the sample surface morphology was investigated using a scanning force microscope (SFM, *Bruker*) in tapping mode.

The SFM height images on the bare ITO and on the modified ITO samples are reported in Figure 1-c. The typical grain-like surface of ITO is clearly visible for all the samples, and from the height images (as well as from the phase, not shown) no morphological difference are detectable. The root mean square of the surface roughness (ρ) is reported above the images. With respect to the bare ITO, the roughness is slightly higher upon SAM treatment, still being within the instrument tolerance (1 nm). This indicates that the employed molecules at the ITO surface forms a molecularly thin film on ITO.

The uniformity of the SAM coverage was tested by a Kelvin probe scanning force microscopy (KP-SFM). Figure 1-d displays the obtained spatially resolved electrostatic contact potential difference (CPD) images between the sample (which is virtually grounded) and the metal-coated cantilever used for the measurement. The color code images show homogeneous CPD (refer to bar on the right of the Figure 1-d for the potentiostatic values). The standard deviation calculated by statistical means on the image values is less than 0.05 V for each measurement. The spatial homogeneity of the CPD value proves a uniform SAM formation and no phase separation between OPA and FOPA on the surface. As observed for the CA measurements, also the CPD values result in a linear function of the amount of FOPA on the surface (see below for more details when referring to Figure 2-f).

It is worth mentioning that upon SAM modification §neither the sheet resistance of ITO (measured with a *Jandel* four-point probe system) nor its transparency (measured via UV−vis absorption with a *PerkinElmer Lambda 950*) was influenced (measurements not shown).
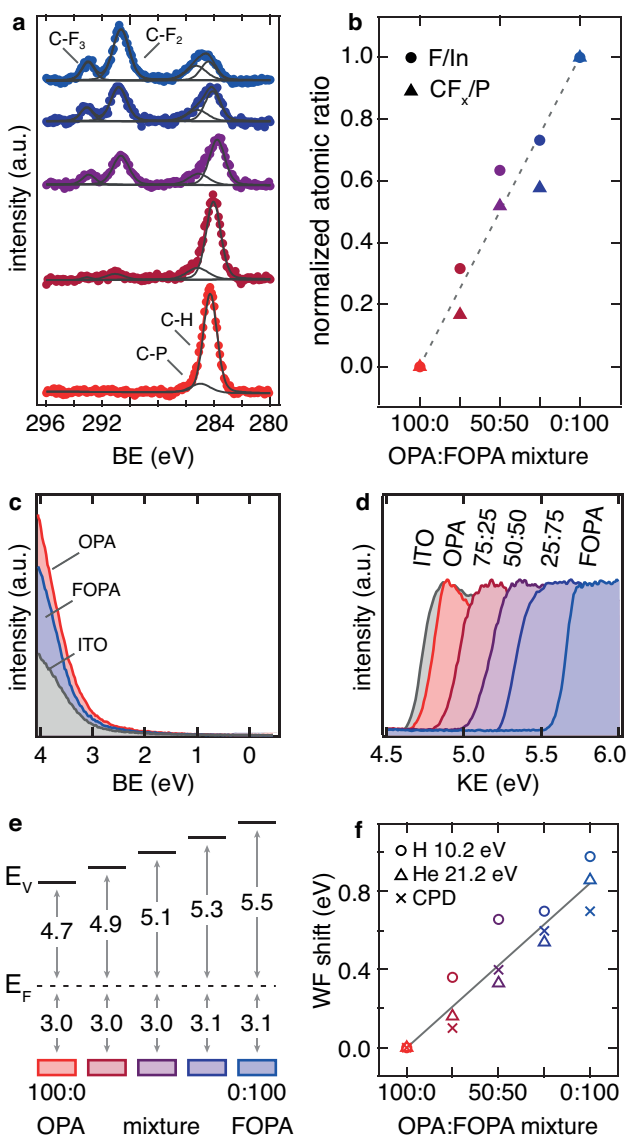
Figure 2. C1s core levels (a) display a continuous increase of the fluorinated components as expected by the nominal OPA:FOPA ratio (bottommost curve refers to 100 % OPA, while the topmost to 100 % FOPA). The nominal mix ratio linearly correlates with the atomic ratio measured via XPS (b). While the VB does not manifest a change between OPA and FOPA (c), the WF increases with increasing FOPA amount in the SAM. The WF shift measured with KP-SFM and UPS are linearly correlated with the OPA:FOPA ratio (f).

X-ray photoelectron spectroscopy (XPS) was performed to obtain an accurate chemical analysis of the mixed SAMs on the ITO.. These measurements can correlate nominal molecular ratio in the solutions with the effective SAM composition on the surface. The XPS spectra were collected in a *JEOL JPS-9030* photoelectron spectrometer system, employing monochromatic Al Kα (1486 eV) as

excitation source. Figure 2-a displays the evolution of the C1s spectra recorded on the samples as a function of the increasing amount of FOPA. P2p, F1s, O1s and In3d were also measured (not shown). The curves have been deconvoluted into four pseudo-Voigt peaks: the component located at lower binding energy (BE = 284 eV and 285 eV) correspond to C-H and C-P species, the two peaks located at higher BE (291 eV and 293 eV) correspond to C-F$_2$ and C-F$_3$, respectively.

As expected, the higher the nominal amount of FOPA in the sample, the higher is the intensity of the fluorinated carbon peaks, and the lower is the intensity of the C-H peak. The intensity of the C-P peak remains constant for all the samples in line with the stoichiometry (both OPA and FOPA molecule have only one C atom chemically bonded to P). To evaluate the real ratio between OPA and FOPA in the SAM, the atomic ratio between the sum of the intensity of the C-F peaks and the P2p peak is calculated and reported in Figure 2-b. Furthermore, also the intensity of the F1s is investigated and related to the In3d peak arising from the ITO substrate. The results are also reported in Fig. 2-b. The dashed line serves as guide for the eye. The linearity between the C-F/P and the F/In atomic ratio confirms the non-cumbersome method presented in this work to form mixed SAMs via simple mixing of the two stock solutions.

The effect on the energy levels was also investigated by means of ultraviolet photoemission spectroscopy (UPS). The valence band (VB) region was measured with an Omicron system equipped with a hemispherical energy analyser (*SPECS Phoibos 100*) using the He I resonance line as excitation source. Figure 2-c shows the VB for OPA and FOPA (the VB of the mixed samples are not reported for the sake of clarity, as they do not display noticeable differences). For the 100:0, 75:25, and 50:50, the VB onset is 3.0 ± 0.1 eV. For the 25:75 and 0:100 the VB onset is 3.1 ± 0.1 eV.

The work function (WF) was evaluated by secondary electron cut-off (SECO). This was measured with both the Omicron system (employing He I discharge lamp) and the

JEOL system (employing H Lyman-α lamp from *Excitech*).[21] The SECO spectra were collected with the samples biased at −10 V to clear the analyser WF. Figure 2-d reports the summary of the measured values for the bare and the functionalised ITO. The WF of the bare ITO substrate resulted to be 4.7 ± 0.1 eV. While OPA does not contribute to any change in the ITO WF, the higher the relative amount of FOPA the higher is the WF. The largest WF (5.5 ± 0.1 eV) is achieved with a 100 % FOPA SAM. The continuous surface work function change is achieved via the control of the surface dipole induced by the employment of OPA and FOPA, which carry intrinsic dipoles pointing in opposite directions.[4]

Combining the information from the VB and the SECO it is possible to schematically depict the energy level alignment. This is reported in Figure 1-e. Furthermore, the variation of the work functions in combination with the unaffected VB demonstrates that the SAM mixture strictly tunes the interface dipole, without creating additional states at the interface.

The dependency between the WF modification induced by the SAM mixture on the ITO with respect to the WF of ITO is reported in Figure 2-f. This figure summarises the data acquired with both photoemission system as well as obtained by means of CPD. The line which is obtained from a fit demonstrate the linearity between the WF shift and the relative amount of FOPA.

To evaluate the effect of the ITO WF tuning in working devices, a series of OLEDs were fabricated. The devices are based on the prototypical small molecule stack comprising α-naphthylphenyl-biphenyl-diamine (NPB) and tris(8-hydroxyquinolino)-aluminum(III) (Alq$_3$). On prepatterned ITO substrates modified with SAMs, the molecules were sequentially evaporated in a vacuum chamber (5×10^{-6} mbar) through shadowing masks. The evaporation occurred simultaneously on all the samples, hence the thickness can be considered equal among all the samples.The final thickness is 60 nm for each film. The cathode deposition of Ca (3 nm) capped with Al (150 nm) followed without breaking the vacuum. Figure 3-a and b
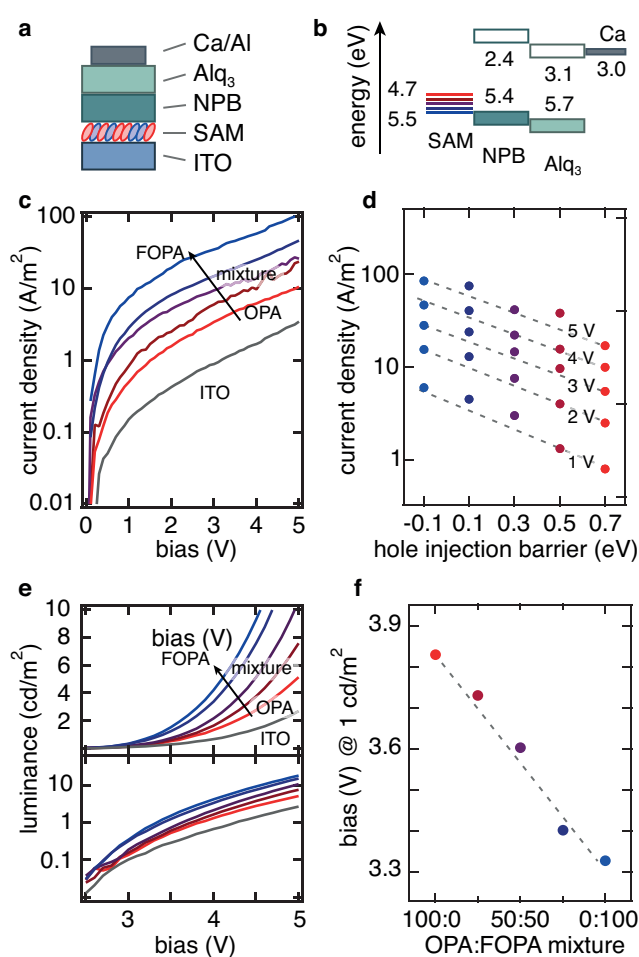

Figure 3. Schematic device OLED stack in (a) with the corresponding energy levels in the device in (b). The OLEDs were characterized by means of *J–V* (c) and luminance vs bias. Hereby a dependency of the current on the hole injection barrier is found (d) according to the Richardson-Schottky model. The *L–V* curves (e) demonstrate that the luminescence onset (1 cd/m^2) correlates linearly with the SAM mixture (f).

show schematically the device architecture and the energy level alignment,[7,22–26] respectively. For the characterization of the OLED devices, current density vs. voltage (*J–V*) and luminance vs. voltage (*L–V*) characteristics were recorded employing a (*Keithley 2450*) source measurement unit, together with a (*Konica Minolta LS-160*) luminance meter in a custom setup.

The *J–V* characteristics of these devices are plotted in Figure 3-c. The devices show a poor diodic characteristic and rather a carrier-only device behaviour. As displayed by the evolution of the current density curves, the higher the

amount of FOPA in the SAM (reflected in high WF), the higher is the current density measured in the devices.

Given the position of the HOMO of NPB which lies at 5.5 eV (see Fig. 3-b), the hole injection barrier (HIB) is decreased by increasing the FOPA in the SAM and hence enhances the hole injection from the modified ITO anode into NPD. To better assess the effect of the continuous tuning obtained by mixing SAMs to modify the WF of ITO, one can analyse the hole injection process. Carrier injection occurring at electrodes has been explained through the Richardson-Schottky thermionic emission model. According to the theory, the current density in the device is determined by the charge injection barriers at the interface. With this model, the injected current density J_{RS} is analytically given by the equation

$$J_{RS} = AT^2 \exp\left(-\frac{\Delta_{HIB}}{k_B T}\right)\left[\exp\left(-\frac{qV}{k_{BT}T}\right) - 1\right]$$

where A is the Richardson-constant, Δ_{HIB} the hole injection energy barrier, T the temperature, k_B the Boltzmann-constant, q the elementary charge and V the voltage bias. The equation shows the paramount impact of Δ_{HIB} on the device performance, and predict a linear correlation between $\ln(J)$ and Δ_{HIB} (at constant temperature and voltage bias). Values from Figure 1-c have been extracted and reported in Figure 3-d, where the $\ln(J)$ is plotted as a function of Δ_{HIB} for five arbitrary chosen values of voltage bias (1 V, 2 V, 3 V, 4 V and 5 V). Δ_{HIB} is calculated as difference between the HOMO of NPB and the WF value of the SAM modified ITO measured via UPS (see Fig. 2-e). The guides for the eye demonstrate the linearity between the HIB and $\ln(J)$ in agreement with the expected Richardson-Schottky thermionic emission behaviour.

The improved carrier injection is also manifested in the device luminescence. Figure 3-e displays the $L-V$ characteristic of the devices in linear (topmost) and semi-log (bottommost) plot. As for the $J-V$ characteristic, the higher the amount of FOPA in the SAM (hence the injected carriers), the higher is the emitted light. This is more clearly displayed by the decrease of the optical turn-on voltage (measured at 1 cd/m^2) displayed in Figure 3-f.

In conclusion, we demonstrated, that the WF of ITO is freely tuneable over a range from 4.7 eV up to 5.5 eV by the functionalization with a corresponding mixed SAM of OPA and FOPA. This provides an effective way to reduce the hole injection barrier in organic optoelectronic devices and is proved in a prototypical OLED structure. Furthermore, the characterization of the mixed SAM revealed that the VB stays unaffected by the SAM treatment, demonstrating that only the interface dipole is tuned.

This approach for modifying electrodes by employing mixed molecules at the interface provides a simple access to a large window of achievable work function in order to better match the energy level of the organic active materials in devices and hence overcomes the need to design specific molecules for this purpose. Furthermore, mixing molecules with opposite dipole direction will allow to continuously tune the work function above and below the intrinsic value of the bare electrode.

The data that support the findings of this study are available from the corresponding author upon reasonable request.

References

[1] K.L. Chopra, S. Major, and D.K. Pandya, Thin Solid Films **102**, 1 (1983).

[2] R. Schlaf, H. Murata, and Z.H. Kafafi, J. Electron Spectros. Relat. Phenomena **120**, 149 (2001).

[3] A.P. Kulkarni, C.J. Tonzola, A. Babel, and S.A. Jenekhe, Chem. Mater. **16**, 4556 (2004).

[4] S. a Paniagua, P.J. Hotchkiss, S.C. Jones, S.R. Marder, A. Mudalige, F.S. Marrikar, J.E. Pemberton, and N.R. Armstrong, J. Phys. Chem. C **112**, 7809 (2008).

[5] S.L. Lai, M.Y. Chan, C.S. Lee, and S.T. Lee, J. Appl. Phys. **94**, 7297 (2003).

[6] Q. Xu, J. Ouyang, Y. Yang, T. Ito, and J. Kido, Appl. Phys. Lett. **83**, 4695 (2003).

[7] Y.J. Pu, G. Nakata, F. Satoh, H. Sasabe, D. Yokoyama, and J. Kido, Adv. Mater. **24**, 1765 (2012).

[8] M.G. Helander, Z.B. Wang, and Z.H. Lu, Org. Electron. **12**, 1576 (2011).

[9] M.G. Helander, Z.B. Wang, J. Qiu, M.T. Greiner, D.P. Puzzo, Z.W. Liu, and Z.H. Lu, Science (80-.). **332**, 944 (2011).

[10] I. Lange, S. Reiter, M. Pätzel, A. Zykov, A. Nefedov, J. Hildebrandt, S. Hecht, S. Kowarik, C. Wöll, G. Heimel, and D. Neher, Adv. Funct. Mater. **24**, 7014 (2014).

[11] M. Timpel, M.V.V.M. V. Nardi, G. Ligorio, B. Wegner, M. Paetzel, B.B. Kobin, S. Hecht, N. Koch, M. Pätzel, B.B. Kobin, S. Hecht, and N. Koch, ACS Appl. Mater. Interfaces **7**, 11900 (2015).

[12] M. Timpel, H. Li, M. V Nardi, B. Wegner, J. Frisch, P.J. Hotchkiss, S.R. Marder, S. Barlow, J. Brédas, and N. Koch, Adv. Funct. Mater. (2017).

[13] S.A. Paniagua, A.J. Giordano, O.L. Smith, S. Barlow, H. Li, N.R. Armstrong, J.E. Pemberton, J.-L. Brédas, D. Ginger, and S.R. Marder, Chem. Rev. **116**, 7117 (2016).

[14] M. Timpel, M. Nardi, and S. Krause, Chem. Mater. 1 (2014).

[15] E. Sauter, C.O. Gilbert, J.F. Morin, A. Terfort, and M. Zharnikov, J. Phys. Chem. C **122**, 19514 (2018).

[16] K. Wu, S. Yu, and Y. Tao, **25**, 6232 (2009).

[17] M. Timpel, M.V. Nardi, S. Krause, G. Ligorio, C. Christodoulou, L. Pasquali, A. Giglia, J. Frisch, B. Wegner, P. Moras, and N. Koch, Chem. Mater. **26**, (2014).

[18] Q. Wang, G. Ligorio, V. Diez-Cabanes, D. Cornil, B. Kobin, J. Hildebrandt, M.V. Nardi, M. Timpel, S. Hecht, J. Cornil, E.J.W. List-Kratochvil, and N. Koch, Adv. Funct. Mater. **28**, 1800716 (2018).

[19] Q. Wang, V. Diez-Cabanes, S. Dell'Elce, A. Liscio, B. Kobin, H. Li, J.-L. Brédas, S. Hecht, V. Palermo, E.J.W. List-Kratochvil, J. Cornil, N. Koch, and G. Ligorio, ACS Appl. Nano Mater. **2**, 1102 (2019).

[20] G. Ligorio, G.F. Cotella, A. Bonasera, N.Z. Morales, G. Carnicella, B. Kobin, Q. Wang, N. Koch, S. Hecht, E.J.W. List-kratochvil, and F. Cacialli, Nanoscale (2020).

[21] A.M. Boehm, J. Wieser, K. Butrouna, and K.R. Graham, Org. Electron. Physics, Mater. Appl. **41**, 9 (2017).

[22] A. Wan, J. Hwang, F. Amy, and A. Kahn, Org. Electron. Physics, Mater. Appl. **6**, 47 (2005).

[23] M. Kröger, S. Hamwi, J. Meyer, T. Riedl, W. Kowalsky, and A. Kahn, Org. Electron. Physics, Mater. Appl. **10**, 932 (2009).

[24] M. Muccini, M. Brinkmann, G. Gadret, C. Taliani, N. Masciocchi, and A. Sironi, Synth. Met. (2001).

[25] A. Curioni, W. Andreoni, R. Treusch, F.J. Himpsel, E. Haskal, P. Seidler, C. Heske, S. Kakar, T. Van Buuren, and L.J. Terminello, Appl. Phys. Lett. (1998).

[26] M. Ben Khalifa, D. Vaufrey, and J. Tardy, Org. Electron. Physics, Mater. Appl. **5**, 187 (2004).